Hybrid core-multishell nanowire forests for electrical connector applications

Rehan Kapadia, Hyunhyub Ko, Yu-Lun Chueh, Johnny C. Ho, Toshitake Takahashi, Zhenxing Zhang, and Ali Javey[a)]

Department of Electrical Engineering and Computer Sciences, University of California at Berkeley, Berkeley, California 94705, USA; Berkeley Sensor and Actuator Center, University of California at Berkeley, Berkeley, California 94705, USA; and Materials Sciences Division, Lawrence Berkeley National Laboratory, Berkeley, California 94720, USA

Electrical connectors based on hybrid core-multishell nanowire forests that require low engagement forces are demonstrated. The physical binding and electrical connectivity of the nanowire electrical connectors arise from the van der Waals interactions between the conductive metallic shells of the engaged nanowire forests. Specifically, the nanofibrillar structure of the connectors causes an amplification of the contact area between the interpenetrating nanowire arrays, resulting in strong adhesion with relatively low interfacial resistance. The nanowire electrical connectors may enable the exploration of a wide range of applications involving reversible assembly of micro- and macroscale components with built-in electrical interfacing. © 2009 American Institute of Physics. [DOI: 10.1063/1.3148365]

As the active areas of systems scale down, physical and electrical connectors based on conventional paradigms fail to provide the necessary performance due to issues of scalability.[1,2] Conventional reusable electrical connectors lack scalability due to separate mechanisms for electrical contact and physical engagement[3] or connector geometries that present significant challenges when scaling to submillimeter regimes.[4,5] Synthetic gecko adhesives and other technologies that rely on chemical interactions can maintain adhesive performance down to the micro- to nanoscale,[6–12] but lack the selectivity necessary for electrical connectors, which require contact between specific components in a system. Recently, hybrid core-shell nanowire (NW) forests were used to fabricate self-selective connectors that required low engagement/disengagement forces.[13] Here, we demonstrate *electrical* connectors based on hybrid core-multishell NW forests that use the same active area for electrical contact and physical adhesion and require low engagement forces. The multishell structure allows control of both the shear adhesion and the electrical properties. The strong shear adhesion of the connectors is due to the large contact area caused by interpenetration of the engaged NW forests, while the electrical connectivity is due to physical contact of the conductive outer shells. Thus, low engagement force electrical connectors with controllable adhesive and electrical properties are demonstrated.

The NW electrical connectors are composed of hybrid core-multishell NW forests on silicon substrates, as illustrated in Fig. 1(a). Ge NW forests were first grown by vapor-liquid-solid method to make high-aspect-ratio nanofibrillar structures.[13,14] The density of the NW forests was $10–20$ NWs/μm^2 at the base and $1–2$ NWs/μm^2 at the canopy. Next, parylene shells with varying thickness $t_p = 50–300$ nm were deposited on the Ge NW forests through gas phase deposition. Finally, a conformal silver shell with thickness $t_{Ag} = 45$ nm was deposited via sputtering. The con-

formal coating of parylene and silver layers is confirmed by transmission electron microscopy (TEM) analyses of individual NWs [Figs. 1(b)–1(d)]. A scanning electron microscopy (SEM) image of a typical NW forest is shown in Fig. 1(c), clearly indicating the mainly vertical orientation and the uniform thickness of the NWs. Each of the components plays an essential role in achieving the desired functionality of NW electrical connectors. The Ge core (modulus $\sim 100–150$ GPa) (Ref. 15) provides the following: (i) a template upon which the shells can be deposited and (ii) prevents aggregation and/or collapse of the resulting high aspect ratio structures. The parylene inner shell enhances the surface compliance of the NW forests, therefore, increasing the total contact area and enhancing the adhesion. The Ag shell
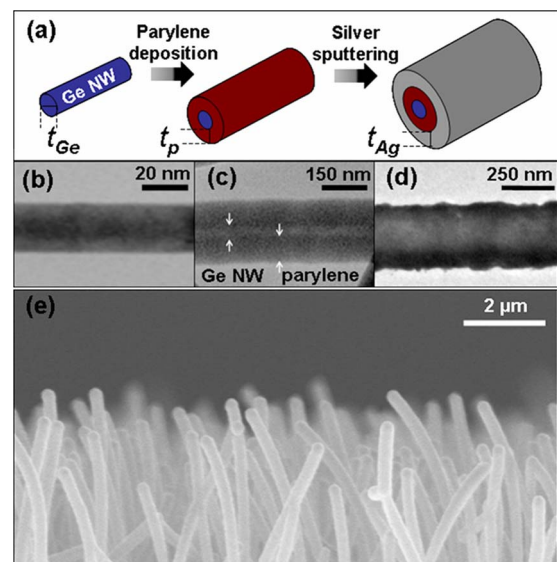

FIG. 1. (Color online) Ge/parylene/Ag core-multishell hybrid NW forests. (a) Illustration of the process flow used to fabricate the core-multishell NW forests. TEM images of (b) Ge NW, (c) Ge/parylene core/shell NW, and (d) Ge/parylene/Ag core-multishell NW. (e) SEM image of a representative core-multishell NW forest.
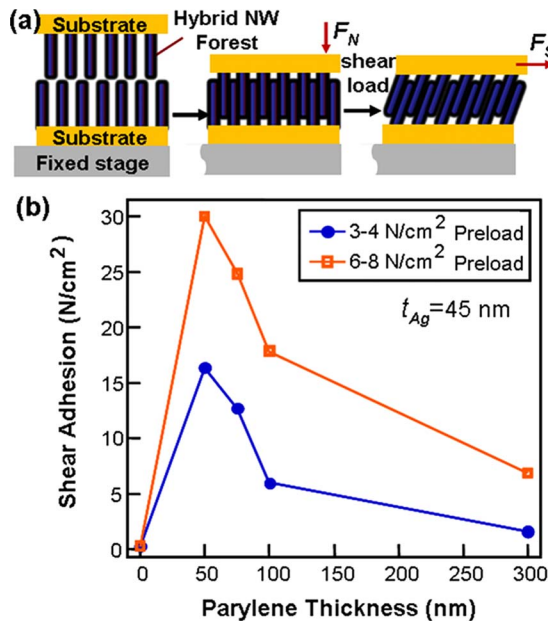
a)Electronic mail: ajavey@eecs.berkeley.edu.

FIG. 2. (Color online) Macroscopic shear adhesion tests of NW electrical connectors. (a) Illustration of the method used to measure the shear adhesion strength. (b) Shear adhesion strength as a function of parylene shell thickness, t_p. Here, the silver shell thickness is maintained constant at t_{Ag} ~ 45 nm.

FIG. 3. (Color online) The calculated contact width between two parallel NWs with 5 μm overlap under a normal force of 200 nN (blue curve). The calculated FF (orange curve) as a function of t_p is also shown. Vertical NW density of 2 NWs/μm^2 is assumed.

is required to enable electrical interfacing between the engaged NW forests.

The macroscale shear adhesion of the NW electrical connectors was tested by first applying a normal preload force F_N to engage the connectors followed by the application of a shear force, F_S [Fig. 2(a)]. This procedure was repeated with increasing F_S until the connectors separated. The shear adhesion strength corresponds to the maximum F_S held without failure. To demonstrate the importance of the parylene shell, we systematically studied shear adhesion as a function of t_p at a constant $t_{Ag}=45$ nm [Fig. 2(b)]. The shear adhesion of NW connectors without parylene coating is <0.8 N/cm^2, while a parylene coating of $t_p=50$ nm increases the shear strength to ~ 30 N/cm^2 for a preload force of ~ 6.5 N/cm^2. This drastic enhancement of the shear adhesion strength with t_p is explained by an increase in the contact area between the engaged NW forests, resulting in increased van der Waals interactions. The contact area between two parallel core-multishell NWs as a function of t_p can be calculated by using Johnson–Kendall–Roberts mechanics.[16] In detail, $P=\pi w^2 E_{NW}/[16R_{NW}(1-\nu^2)]-[\pi w W E_{NW}/2(1-\nu^2)]^{0.5}$ was used to find the contact width w as a function of t_p, where P is the applied normal force per unit length, W is the work of adhesion, E_{NW} is the effective Young's modulus of the NWs, and R_{NW} is the radius of the NWs. The radius R_{NW} is the sum of the thicknesses of the three materials, $R_{NW}=t_{Ge}/2+t_p+t_{Ag}$. The effective Young's modulus of the NWs was calculated by using $1/E_{NW}=[t_{Ge}/(2E_{Ge})+t_p/E_p+t_{Ag}/E_{Ag}] \times (1/R_{NW})$ with $E_{Ge}=103$ GPa, $E_p=2.8$ GPa, and $E_{Ag}=78$ GPa. The Poisson's ratio ν was taken to be 0.35. The increase in contact area with t_p is clearly illustrated in Fig. 3 for two parallel NWs with $t_{Ge}=30$ nm and $t_{Ag}=45$ nm, overlapping by 5 μm under a 200 nN normal force. The results demonstrate the importance of parylene inner shell in achieving enhanced contact area[13] despite the fact that the polymeric shell is covered with an outer silver layer.
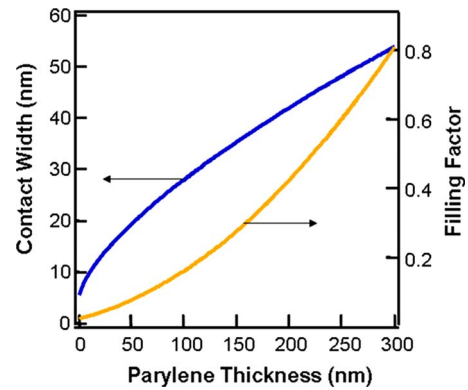
A decrease in the shear adhesion is observed for t_p >50 nm [Fig. 2(b)]. This trend is attributed to a decrease in interpenetration depth (i.e., total contact area) for a given F_N due to an increase in the filling factor (FF) of the NW forests. The FF is estimated by using FF=$(\pi R^2 \times \text{total \# of NWs})/(\text{total area})$, assuming perfectly vertical NWs (Fig. 3). Therefore, increasing t_p results in two competing effects—an increase in the surface compliance and an increase in the FF, resulting in the observed shear adhesion trend with a peak at $t_p \sim 50$ nm. Our previous work on NW connectors also shows a similar trend.[13]

To further depict the importance of the parylene inner shell for obtaining high adhesion strength, control tests were carried out with $t_p=0$ nm while systematically increasing t_{Ag} from 45 to ~ 300 nm. In all cases, the adhesion was <2 N/cm^2 at a preload of ~ 4 N/cm^2. This low shear adhesion for NW connectors without a parylene coating clearly demonstrates the necessity of the parylene inner shell for achieving high shear adhesion.

The normal preload force (F_N) applied also affects the shear adhesion. As can be seen in Fig. 2(b), an increase in the shear adhesion is observed with increasing F_N. This trend is attributed to the greater interpenetration depth of the NW forests with larger preload, resulting in higher effective contact area. Finally, the NW connectors provide highly specific binding with low adhesion to nonself-similar surfaces (e.g., glass, planar parylene coated surfaces, and cloth) as previously demonstrated.[13] This is due to the relatively high stiffness of the NW connectors as compared to those used in synthetic gecko[12] adhesives. As a result, small contact area and low adhesion is observed when engaged with nonself-similar surfaces. This selective adhesion is an important and highly desired characteristic of a connector technology.

In addition to the strong adhesion capabilities, the connectors are also electrically active due to the silver outer shell. The performance of NW electrical connectors was investigated by measuring the electrical resistance in the engaged mode [Fig. 4(a)]. The nominal contact area between the engaged connectors was ~ 25 mm^2. By applying voltages from 0 to 0.5 V, I-V curves were generated and the resistance was directly extracted. A representative I-V characteristic for $t_p=100$ nm and $t_{Ag}=45$ nm NW connector is shown in the inset of Fig. 4(a), exhibiting ohmic behavior over the entire range of measurement. The resistance of the
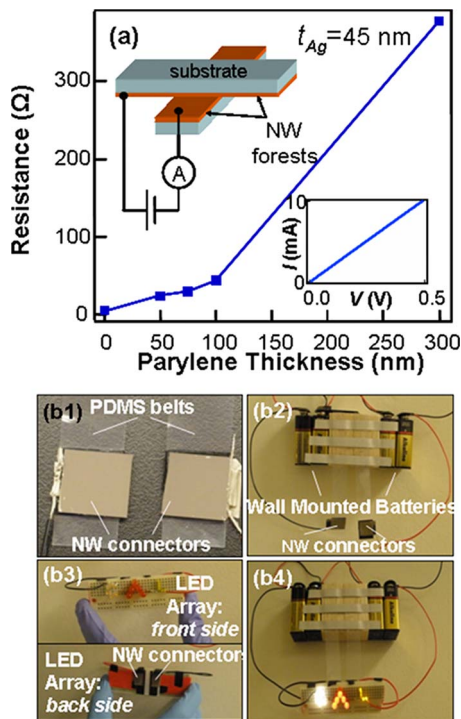
FIG. 4. (Color online) Electrical properties of the NW connectors. (a) Measured resistance as a function of t_p for connectors with ~25 mm² overlap. The inset shows the setup used to measure the resistance. A representative I-V curve for engaged connectors with t_p=100 nm and t_{Ag}=45 is also shown. (b1) NW electrical connectors are attached to two PDMS belts and (b2) electrically connected to a wall mounted battery array. (b3) Two complementary connectors are also attached to the back of an LED array. (b4) Once the connectors are engaged, the LED array is physically and electrically connected to the battery array, demonstrating the macroscale operation of the NW electrical connectors (enhanced online). [URL: http://dx.doi.org/10.1063/1.3148365.1]

engaged connectors as a function of t_p [Fig. 4(a)] clearly indicates that the resistance of the connectors is not limited by the contact area between NW forests. Instead, the overall resistance is dominated by the parasitic resistances across the individual NW forests. To characterize the parasitic resistance, resistance across a single NW forest was measured as a function of length. For a connector of width ~5 mm, t_p =100 nm, and t_{Ag}=45 nm, the resistance per mm length scale was ~3 Ω/mm. This is attributed to the relatively thin Ag films used in this work. In particular, the Ag coating at the base of the NW forests is expected to decrease in thickness when thicker parylene films are used, which is consistent with the observed resistance versus t_p trend [Fig. 4(a)]. In the future, further materials optimization is necessary to reduce the parasitic resistance across the NW forests.

As a demonstration of a potential application of NW connectors, an light-emitting diode (LED) array was connected to a wall-mounted battery array both physically and electrically by using NW electrical connectors [Fig. 4(b); See EPAPS supplementary material at [URL] for video of demonstration]. Two connectors were attached to the ends of two

polydimethylsiloxane (PDMS) belts [Fig. 4(b)1], each of which was then connected to the negative and positive ends of a battery array [Fig. 4(b)2]. Two additional connectors were attached to the back of an LED array and were electrically connected to the positive and negative ends [Fig. 4(b)3]. By engaging the NW electrical connectors, the LED array was physically and electrically connected to the battery array [Fig. 4(b)4]. The engaging and disengaging was repeated multiple times [Fig. 4(b), supplementary video].

In conclusion, physical adhesion with built-in electrical interfacing is demonstrated by using hybrid core-multishell NW connectors. NW connectors allow for highly specific binding with low engagement forces arising from their nanofibrillar structure. The multishell configuration is required to simultaneously provide both the necessary surface compliance and electrical conductivity. Uniquely, the use of multicomponent NWs allows for the precise control and engineering of the connector properties, a feature that is attractive for making connectors optimally suited for a wide range of technological applications.

[1] M. Yim, Y. Zhang, K. Roufas, D. Duff, and C. Eldershaw, IEEE/ASME Trans. Mechatron. **7**, 442 (2002).

[2] M. B. Cohn, K. F. Böhringer, J. M. Novorolski, A. Singh, C. G. Keller, K. Y. Goldberg, and R. T. Howe, Proc. SPIE **3511**, 2 (1998).

[3] B. Chan and P. Singh, Proceedings of the 46th IEEE Electronic Components and Technology Conference, 1996 (unpublished), p. 460.

[4] *Electrical Contacts: Principles, and Applications*, edited by P. G. Slade (Dekker, New York, 1999).

[5] M. Braunovic, V. Konchits, and N. Myshkin, *Electrical Contacts: Fundamentals, Applications and Technology* (CRC, Boca Raton, 2007).

[6] E. Arzt, S. Gorb, and R. Spolenak, Proc. Natl. Acad. Sci. U.S.A. **100**, 10603 (2003).

[7] M. Murphy, B. Aksak, and M. Sitti, J. Adhes. Sci. Technol. **21**, 1281 (2007).

[8] Y. Zhao, T. Tong, L. Delzeit, A. Kashani, M. Meyyappan, and A. Majumdar, J. Vac. Sci. Technol. B **24**, 331 (2006).

[9] L. Qu and L. Dai, Adv. Mater. (Weinheim, Ger.) **19**, 3844 (2007).

[10] L. Ge, S. Sethi, L. Ci, P. M. Ajayan, and A. Dhinojwala, Proc. Natl. Acad. Sci. U.S.A. **104**, 10792 (2007).

[11] J. Lee, R. S. Fearing, and K. Komvopolous, Appl. Phys. Lett. **93**, 191910 (2008).

[12] K. Autumn, Y. A. Liang, S. T. Hsieh, W. Zesch, W.-P. Chan, W. T. Kenny, R. Fearing, and R. J. Full, Nature (London) **405**, 681 (2000).

[13] H. Ko, J. Lee, B. E. Schubert, Y.-L. Chueh, P. W. Leu, R. S. Fearing, and A. Javey, Nano Lett. **9**, 2054 (2009).

[14] A. Javey, ACS Nano **2**, 1329 (2008).

[15] L. T. Ngo, D. Almécija, J. E. Sader, B. Daly, N. Petkov, J. D. Holmes, D. Erts, and J. J. Boland, Nano Lett. **6**, 2964 (2006).

[16] K. L. Johnson, K. Kendall, and A. D. Roberts, Proc. R. Soc. London, Ser. A **324**, 301 (1971).